Special issue article

Journal of Physical Organic Chemistry

Received: 25 October 2015, Revised: 19 April 2016, Accepted: 25 April 2016, Published online in Wiley Online Library: 31 May 2016

(wileyonlinelibrary.com) DOI: 10.1002/poc.3587

Vibrational spectra, conformational properties and argon matrix photochemistry of diacetyl diselenide, $CH_3C(O)Se_2C(O)CH_3$ †

Jovanny A. Gómez Castaño[a,b]*, Rosana M. Romano[a], Ana R. Salamanca[b], Germán Amésquita[c], Helmut Beckers[d], Helge Willner[d] and Carlos O. Della Védova[a]

By oxidation of selenoacetic acid, $CH_3C(O)SeH$, we have prepared the hitherto unknown diacetyl diselenide, $[CH_3C(O)Se]_2$. Its vibrational properties were studied experimentally, both in neat liquid (Fourier transform infrared spectroscopy and Raman) with the molecule isolated in argon matrix at low temperatures and theoretically using MP2 and B3LYP methods in combination with 6-31+G(d), 6-311++G(3df,3dp) or aug-cc-pvDZ basis sets. Analysis of Ar matrix spectra reveals a conformational equilibrium in gas phase at room temperature, which was interpreted by considering only two of the three stable rotamers predicted by our three-dimensional potential energy surface scans. Energetic properties of three minima found theoretically were further studied in terms of donor–acceptor interactions by using natural bond orbital calculations at the same levels of theory. From this, it was possible to rationalize the conformational stability order and molecular structures by means of vicinal hyperconjugative delocalizations involving lone pairs on selenium or oxygen atoms and C=O, C–C or Se–C antibonding orbitals. The photochemistry of the compound in the argon matrix in the range between 200 and 800 nm was also investigated, revealing only one photochemical path to produce ketene, $H_2C{=}C{=}O$, methylselane, CH_3SeH, and carbonyl selenide, OCSe. Copyright © 2016 John Wiley & Sons, Ltd.

Keywords: diselenide; hyperconjugation; matrix photochemistry; NBO; photodecomposition

INTRODUCTION

Diselenides, RSeSeR, are a versatile group of substances used as precursors of a wide variety of new selenium compounds. Their biological and medicinal properties are also of interest, mainly because of their antioxidant, biocatalytic, antiparasitic, neuronal and analgesic effects.[1–10] Chemical applications of diselenides arise mainly from the convenient inclusion of RSe units in both organic and inorganic synthesis by cleavage of the Se–Se bond; this is mostly influenced by the weaker dissociation energy of this bond in comparison with C–Se, H–Se and S–S bonds.[11] Representative members of this family include $(SePh)_2$ and $(CH_3Se)_2$, which are compounds widely employed in organic reactions and catalysis because of the high yields achieved (>90%) for the inclusion of PhSe – and CH_3Se – moieties, respectively.[12–19]

On the other hand, bis(R-carbonyl)diselenides, RC(O)SeSeC(O)R, reported to date correspond to compounds with aromatic (R–) substituents rather than aliphatic analogs, probably because of a higher thermal stability of aromatic species. Among the few reports of the aliphatic derivatives, the molecule $[Me_2NC(O)Se]_2$, for example, was used by Gong *et al.*, as the starting reagent to obtain a series of new compounds of general formula $Me_2NC(O)SeRSeC(O)NMe_2$.[20] Wang *et al.* synthesized a series of new diselenides $[RC(O)Se]_2$ (R = aromatic groups) through the corresponding carbonyl benzoyl chloride, RC(O)Cl[21], and later, Kumar *et al.* used a similar procedure to prepare the first bis(ferrocene carbonylselenide), $[FcC(O)Se]_2$, using ferrocene (Fc) Se-carboxylic acid, FcC(O)SeH, as starting reagent.[22] More recently however, Takahashi *et al.* obtained the identical diselenide by reacting FcC(O)SeH with oxygen.[23]

Oxidation with oxygen has been used by us to obtain the hitherto unknown aliphatic diselenides, $[RC(O)Se]_2$, from novel

* *Correspondence to: Jovanny A. Gómez Castaño, Laboratorio de Química Teórica y Computacional, Grupo de Investigación Química–Física Molecular y Modelamiento Computacional (QUIMOL), Facultad de Ciencias, Universidad Pedagógica y Tecnológica de Colombia (UPTC), Avenida Central del Norte, Tunja, Boyacá, Colombia.*
E-mail: jovanny.gomez@uptc.edu.co

† *This article is published in Journal of Physical Organic Chemistry as a special issue on New Latin American Conference at Villa Carlos Paz, Córdoba, Argentina, 2015 by Elba I. Buján (Universidad Nacional de Córdoba)*

a *J. A. Gómez Castaño, R. M. Romano, C. O. Della Védova*
CEQUINOR (UNLP-CONICET), Departamento de Química, Facultad de Ciencias Exactas, Universidad Nacional de La Plata, 47 esq. 115, 1900, La Plata, Argentina

b *J. A. Gómez Castaño, A. R. Salamanca*
Laboratorio de Química Teórica y Computacional, Grupo de Investigación Química–Física Molecular y Modelamiento Computacional (QUIMOL), Facultad de Ciencias, Universidad Pedagógica y Tecnológica de Colombia (UPTC), Avenida Central del Norte, Tunja, Boyacá, Colombia

c *G. Amésquita*
Grupo de Investigación en Informática, Electrónica y Comunicaciones (INFELCOM), Facultad de Ingenieria, Universidad Pedagógica y Tecnológica de Colombia (UPTC), Avenida Central del Norte, Tunja, Boyacá, Colombia

d *H. Beckers, H. Willner*
Anorganische Chemie, Bergische Universität Wuppertal, Gaußstr. 20, D-42097, Wuppertal, Germany

$$2\ RC(O)SeH + 1/2\ O_2 \rightarrow RC(O)SeSeC(O)R + H_2O$$

Scheme 1. Aliphatic diacetyl diselenides obtained by oxidation of seleno-carboxylic acids

selenocarboxylic acids, RC(O)SeH (R = CH_3, CF_3, CHF_2 and $CClF_2$),[24,25] (refer to Scheme 1).

To the best of our knowledge, neither conformational behavior nor photochemistry of any bis(R-carbonyl) diselenides has been described. As shown in Fig. 1, these structures present three single covalent bonds, allowing possible co-existence of several stable rotational forms (conformers) at room temperature. Such rotamers can be identified by analysis of the IR and Raman spectra and also of low-temperature inert gas matrices. For this purpose, the experimental vibrational frequencies are compared with frequencies obtained from computations of the equilibrium structures established on the potential energy surface. Herein, we report the preparation, vibrational characterization and rotational behavior of bis(acetyl)diselenide, $[CH_3C(O)Se]_2$, as well as its photochemistry in solid argon at 10 K.

EXPERIMENTAL

Diacetyl diselenide, $[CH_3C(O)Se]_2$, was obtained directly by oxidizing a sample of pure selenoacetic acid, $CH_3C(O)SeH$, with dry air during a few minutes in a closed glass vessel at room temperature. In order to avoid further oxidation of the titled compound, the excess air as well as the water formed was pumped off at the vacuum line. The compound was also formed as a by-product during the preparation of selenoacetic acid, $CH_3C(O)SeH$.[24] $[CH_3C(O)Se]_2$ presented as a low volatile, sticky, orange liquid at room temperature with a very fetid and persistent odor. To check its identity, a small sample of the compound was diluted in dry toluene in a dry box under argon atmosphere and injected into an electron impact ionization GC-MS (Shimadzu QP-2010) device. Pure liquid diacetyl diselenide was also handled in a dry argon box to prepare samples for Fourier transform infrared spectroscopy (FTIR) and Raman measurements.

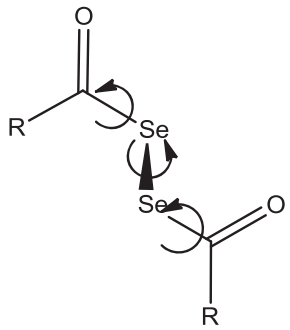

Figure 1. Possible rotations along the C–Se and Se–Se bonds of $[RC(O)Se]_2$

Gaseous mixtures of $[CH_3C(O)Se]_2$ with Ar (AGA) in proportion of ca. 1:1000 were prepared by standard manometric methods and deposited on a cooled CsI window to ca. 10 K by means of a Displex closed-cycle refrigerator (SHI-APD Cryogenics, model DE-202) using the pulse deposition technique.[26–28] The matrix-isolated FTIR spectra were recorded on a Nexus Nicolet instrument equipped with either an Tipe B Mercury Cadmiun Telluride Detector (MCTB) or a deuterated triglycine sulfate (DTGS) detector (for the ranges 4000–400 or 600–180 cm^{-1}, respectively). Following deposition and IR analysis of the resulting matrix, the argon-isolated sample was exposed to broad-band UV-visible radiation ($200 \leq \lambda \leq 800$ nm) from a Spectra-Physics Hg–Xe arc lamp operating at 1000 W. The output from the lamp was directed through a water filter to absorb IR radiation and to minimize any heating effect. The IR spectra of the matrix with resolutions of 0.5 and 0.125 cm^{-1} were then recorded at different times of irradiation in order to monitor closely any change in the spectra.

Quantum chemical calculations were performed with the Linux/UNIX version of Gaussian 09 (Rev. C.01) program,[29] under the TCP Linda parallel execution environment, running on our scalable computational cluster named "**A** **t**eam **o**f **m**ultiprocessors **i**n support of **c**hemical **c**alculations" (Atomicc). This is currently comprised of 20 Intel Xeon processors distributed in five HP workstations (one Z800 and two Z600) and uses an OS platform Suse Linux Enterprise Server 11 SP2. Minima searches were approached by means of a relaxed two-dimensional potential energy surface (PES) scan, constructed by simultaneously varying the two dihedral angles using the B3LYP/6-31+G(d) method. Geometry optimizations were sought using standard gradient techniques by simultaneous relaxation of all the geometrical parameters at B3LYP/6-31+G(d), B3LYP/6-311++G (3df,3dp) and MP2/aug-cc-pvDZ levels of approximation. The calculated vibrational properties correspond in all cases to potential energy minima for which no imaginary vibrational frequency was found. Natural bond orbital (NBO) analysis of wave functions of minima molecular structures was performed using the NBO program 3.1[30] incorporated in Gaussian 09. All the molecular surfaces were obtained with the GaussView 05 program.[31]

RESULTS AND DISCUSSION

Mass spectrum

As can be seen in Fig. 2, the mass spectrum of $[CH_3C(O)Se]_2$ presents a quite simple fragmentation pattern. The most intense

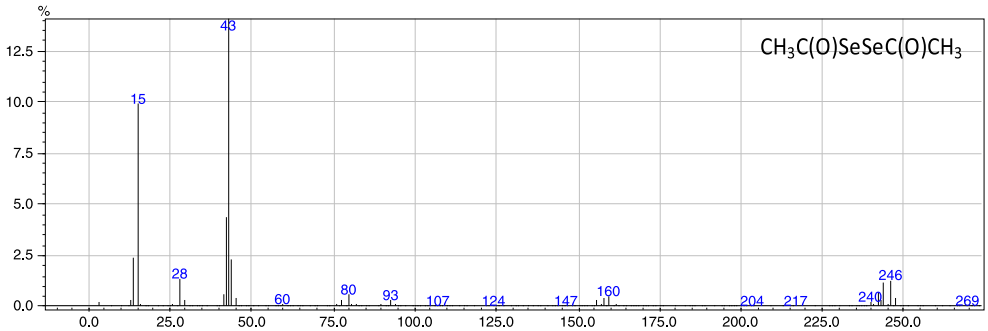

Figure 2. Electron-impact mass fragmentation spectrum of $[CH_3C(O)Se]_2$

peak corresponds to m/z = 43 (CH_3CO^+, 100%), followed by peaks at m/z = 15 (CH_3^+, ~10%), m/z = 28 (CO^+, <2%), m/z = 80 (Se^+, <2%) and 160 (Se_2^+, <2%). The natural isotopic contribution peaks of selenium are also observed at 76, 77, 78 and 82 m/z ratios for one atom (Se^+) and at 152, 154, 156 and 164 m/z ratios for two atoms (Se_2^+). The parent ion is detected at m/z = 246 (<2%), enabling the identity of the titled compound. The mass fragmentation outline of diacetyl diselenide was found to be similar to that reported for diacetyl disulfide, $[CH_3C(O)S]_2$, showing a main peak at m/z = 43 (CH_3CO^+) and molecular ion at m/z = 150 (<2%).[32] The formation of the Se_2^+ fragment and the lack of detection for a mass corresponding to symmetrical cleavage, ($CH_3C(O)Se^+$), could be associated with the unexpected, relatively high stability of the Se–Se bond in the ionized species.

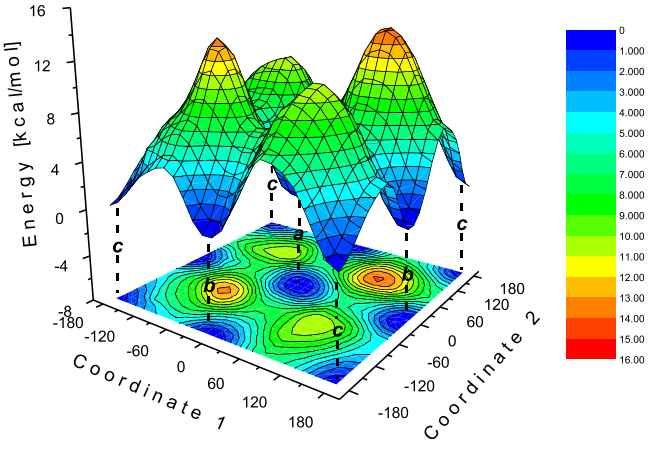

Figure 3. Two-dimensional PES for $[CH_3C(O)Se]_2$ constructed by the variation of [O(9)–C(3)–Se(4)–Se(5)] and [O(10)–C(6)–Se(5)–Se(4)] dihedral angles, coordinates 1 and 2, respectively, calculated at the B3LYP/6-31G (d) approximation level. (For atom numbering, refer to Fig. 4)

Equilibrium structures and energies

Conformational behavior of $[CH_3C(O)Se]_2$ was first approached theoretically by analyzing the energetic effects caused by the simultaneous internal rotation of its two O=C–Se–Se dihedral angles (refer to Fig. 1) at the B3LYP/6-31G(d) level of theory. The CSeSeC dihedral angle was defined as gauche as known for dichalcogenes. The resulting two-dimensional PES (Fig. 3) was constructed allowing one O=C–Se–Se angle to rotate 360° at 10° increments and the other dihedral angle to rotate also in steps of 10°, while performing a geometry optimization to the

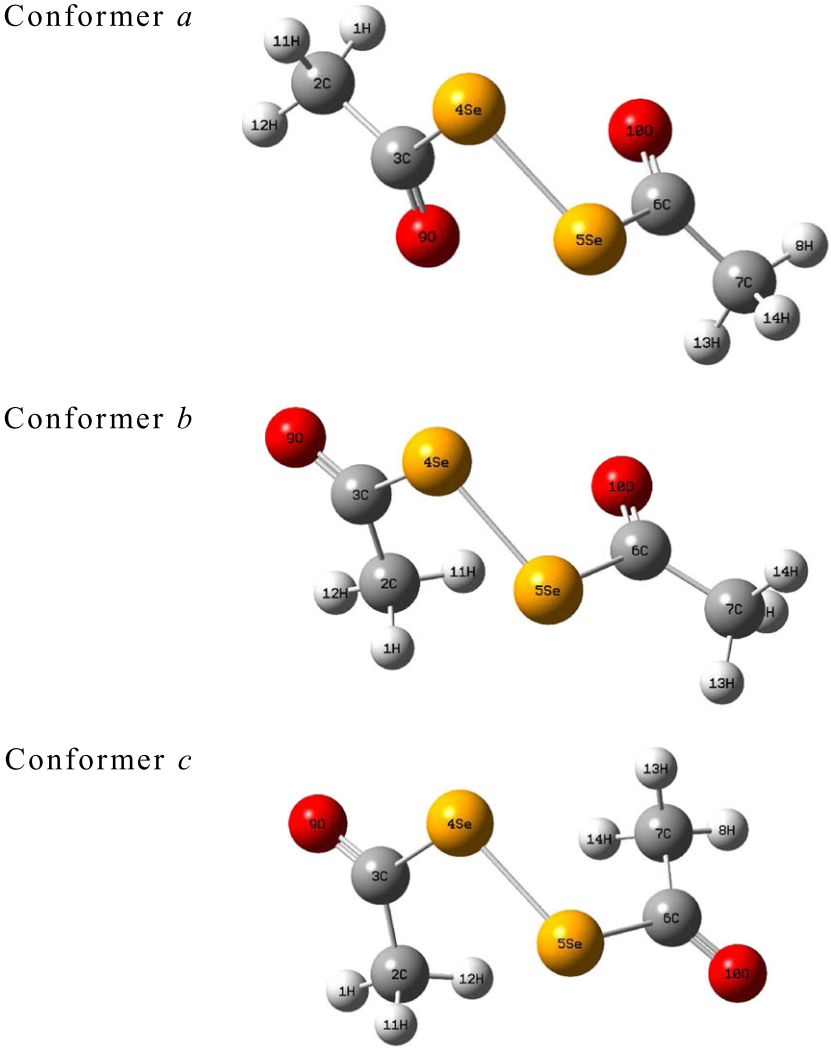

Figure 4. Molecular models of three minima of $[CH_3C(O)Se]_2$ calculated with the MP2/aug-ccpVDZ

rest of the structural parameters at each point (relaxed scan). As can be noted from Fig. 3, three local minima were identified: two of them (both dihedrals equal to 0° and 180°, respectively) showing C_2 symmetry and the third (one dihedral 0° and the other 180°) having C_1 symmetry. Hereinafter, these structures will be called *a*, *c* and *b*, respectively.

The three minima structures were subsequently used as starting points for geometric optimizations and thermochemistry calculations using B3LYP/6-311++G(3df,3pd) and MP2/aug-cc-pvdz levels of theory without constraints. As a result, none of the optimized structures presented imaginary frequencies, and thus, their identities were confirmed as local minima. With both approximations, the conformer *a* was found to be 0.18 and 1.25 kcal/mol (DFT) and 0.42 and 1.31 kcal/mol (MP2 method) lower in energy than conformers *b* and *c*, respectively. Figure 4 shows the optimized molecular models, and Table 1 lists some selected geometrical parameters calculated with MP2/aug-cc-pvdz method for the three conformers. As illustrated in Table 1, an increasing variation in Se–Se bond ($2.321 < 2.334 < 2.344$ Å) and C–Se–Se–C dihedral angle ($63.7° < 76.2° < 86.6°$) was observed among the conformers *a*, *b* and *c*, respectively. As we will explained in the next subsection, this tendency can be rationalized in terms of electron occupancy and anomeric effect.

Introducing the sum of electron and thermal free energies, obtained from thermochemical calculations at 298 K, into the Boltzmann distribution equation, an estimation for gas rotational equilibrium at room temperature of 86% (conf-*a*), 12% (conf-*b*) and 2% (conf-*c*) with the density functional theory method and 74% (conf-*a*), 21% (conf-*b*) and 5% (conf-*c*) with MP2 method was obtained (refer to Table 2).

Table 1. Selected structural parameters of three minima of $[CH_3C(O)Se]_2$ calculated with the MP2/aug-cc-pvdz method using bond lengths and angles measured, respectively, in Angstroms and degrees

Geometry parameter	Conformer		
	a	*b*	*c*
(Se–Se)	2.321	2.334	2.344
Se(4)–C(3)	1.980	1.974	1.975
Se(5)–C(6)	1.980	1.977	1.975
C(3)=O(9)	1.213	1.217	1.218
C(6)=O(10)	1.213	1.215	1.218
C(2)–C(3)	1.513	1.506	1.508
C(6)–C(7)	1.513	1.514	1.508
Se–Se–C(3)	96.1	104.0	103.5
Se–Se–C(6)	96.1	98.2	103.5
Se(4)–C(3)=O(9)	122.9	115.2	115.4
Se(5)–C(6)=O(10)	122.9	122.6	115.4
Se(4)–C(3)–C(2)	111.8	119.0	119.1
Se(5)–C(6)–C(7)	111.8	112.2	119.1
C–Se–Se–C	63.7	76.2	86.6
Se–Se–C(3)–C(2)	173.9	3.9	1.9
Se–Se–C(6)–C(7)	173.9	168.8	1.9

Natural bond orbital analysis

In order to investigate theoretically the origin of energy differences exhibited among the three equilibrium structures and the relationship to their molecular geometries, we performed a sequence of NBO analyses as follows. First, stabilizing effects because of electronic delocalization contributions in each conformer were quantitatively assessed by calculating again the wave function over the optimized structures, but this time deleting all non-Lewis-type NBO from the basis set. Then, a full orbital population analysis was performed to determine the specific donor–acceptor interactions responsible for making conformer *a*, the most stable structure.

According to the calculated energies of deletion, E(L), and the energy change, E(NL), localized contributions favor the structures *b* and *c* over *a* by 6.0 and 10 kcal/mol, respectively (refer to Table SI-1 in Supporting Information). The data in Table SI-1 also demonstrates that the contribution by energetic delocalization, E(NL), in conformer *a* is higher than the localized contribution, E(L), of conformer *c* that is almost the same as the E(L) of conformer *b*. The major stability of conformer *a* can be attributed to its higher electronic delocalization energy.

On the other hand, the main stabilization energies, $\Delta E^{(2)}$, predicted for each structure by the NBO analysis (refer to Table SI-2) indicate that by far, the largest delocalization contributions for all three conformers were found to come from electronic charge transfers. These involve lone pairs on selenium (n_{Se}) or oxygen (n_O) atoms and vicinal antibonding orbitals, according to three principal categories: (1) $n_{Se} \rightarrow \pi^*_{C=O}$; (2) $n_O \rightarrow \sigma^*_{C-C}$; and (3) $n_O \rightarrow \sigma^*_{Se-C}$, each composed of two equal contributions. Whichever category is concerned, the major electronic transfers were always obtained for conformer *a*, followed by those of conformer *b* and then conformer *c*, which is in agreement with the conformational stabilization order predicted initially (Table 2). Figure 5 schematizes the main delocalizing interactions in each conformer by means of NBO overlap diagrams.

Table 2. Energies and relative population distribution at 298 K of three minima of $[CH_3C(O)Se]_2$ calculated at different levels of approximation

Conformer	E_h (hartrees)	ΔE (kcal/mol)	$E_{h0} + G°$ (hartrees)	$\Delta G°$ (kcal/mol)	Population %
Method: B3LYP/6-311++G(3df,3dp)					
a	−5109.73769092	0.00	−5109.685238	0.00	86
b	−5109.73691144	0.18	−5109.683386	1.16	12
c	−5109.73564072	1.25	−5109.681890	2.10	2
Method: MP2/aug-cc-pvdz					
a	−5105.61707688	0.00	−5105.562832	0.00	74
b	−5105.61641043	0.42	−5105.561637	0.75	21
c	−5105.61498619	1.31	−5105.560367	1.55	5

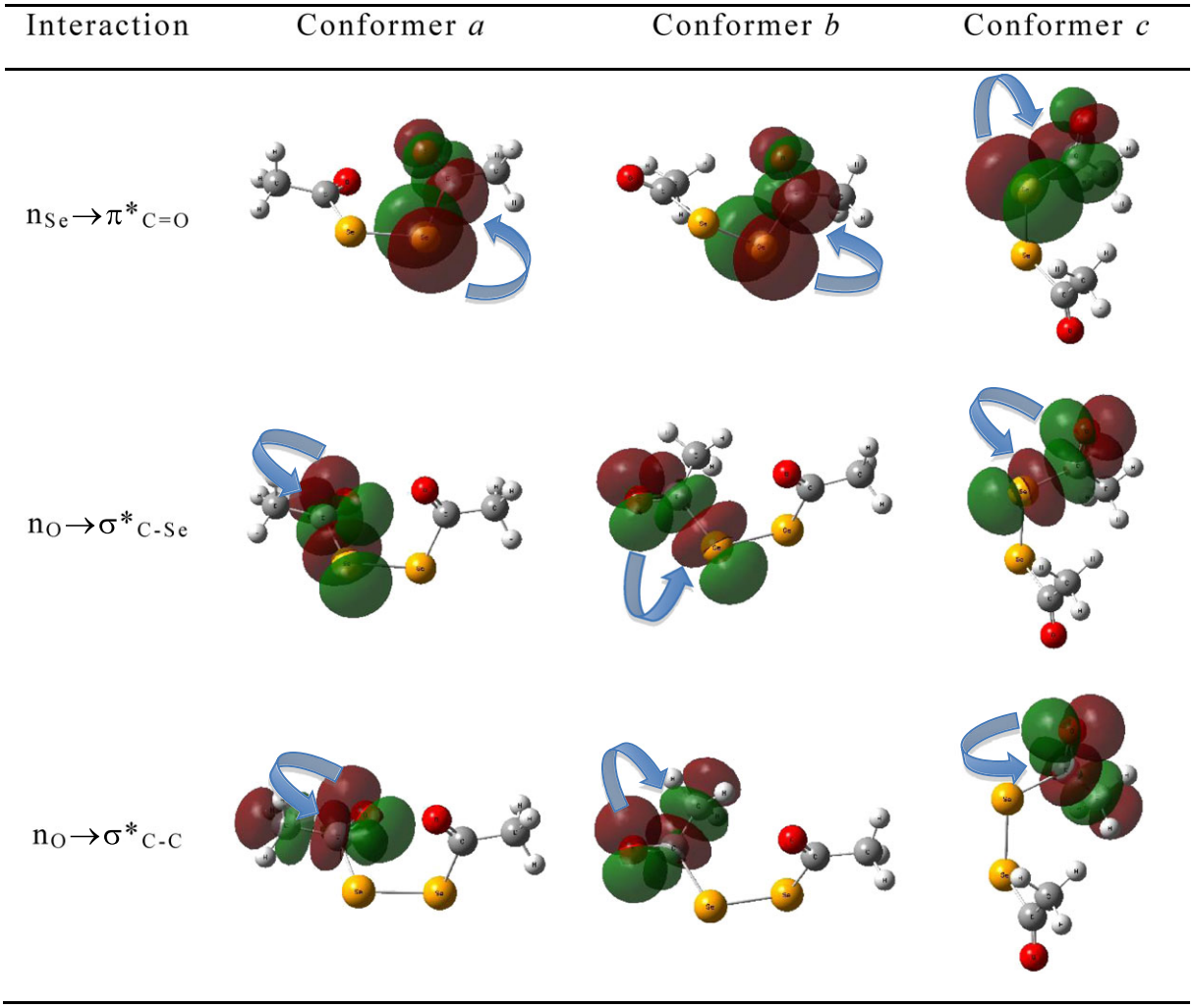

Figure 5. Schematic delocalizing overlaps for conformers *a*, *b* and *c* of $[CH_3C(O)Se]_2$ calculated at the B3LYP/6-311++G(3df, 3pd) level of approximation. Blue arrows indicate direction of charge transference

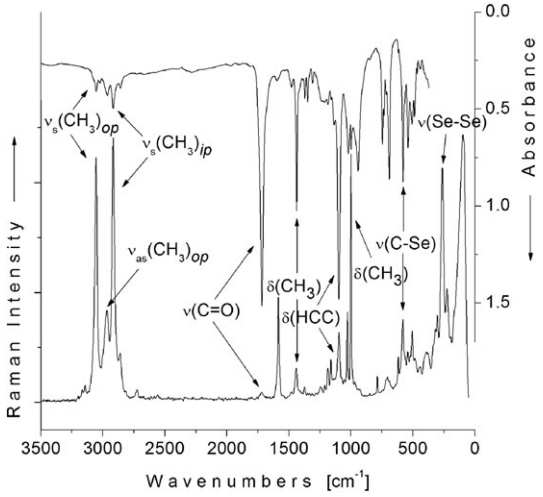

Figure 6. FTIR (top, resolution = 2 cm^{-1}) and FTRaman (bottom, power = 150 mW and resolution of 4 cm^{-1}) spectra of pure liquid of $[CH_3C(O)Se]_2$ measured at room temperature

The NBO analysis also allows us to offer a numerical explanation to the gradual increase (conf. *a* < conf. *b* < conf. *c*) in the geometric parameters Se–Se and C–Se–Se–C (refer to Table 1). In the case of the Se–Se distance, the NBO occupancies calculated over orbital σ_{Se-Se} show a value of 1.98118 in the conformer *a*, followed by values of 1.97880 and 1.97824 in conformers *b* and *c*, respectively; meanwhile, the occupancies over σ^*_{Se-Se} give values of 0.02038 (conf. *a*), 0.03703 (conf. *b*) and 0.04931 (conf. *c*). Thus, the shortest Se–Se length obtained in conformer *a* can be attributed to a greater electron density. Regarding the dihedral angle C–Se–Se–C, its variation among the conformers can be rationalized by considering different grades of the *gauche effect*; this is mainly originated by a charge transference between orbitals n_{Se} and σ^*_{C-Se} (*anomeric effect*). In conformer *c*, the largest value of this transference, 6.71 kcal/mol, is favored because of its wider C–Se–Se–C angle (86.6°); this contrasts to conformers *b* and *a* where their lower charge transferences, 6.21 and 5.41 kcal/mol, respectively, rebound in narrower CSeSeC angles (76.2° and 63.7°).

Table 3. Experimental (IR, Raman and Ar matrix) and theoretical (MP2/aug-cc-pvdz) vibrational wavenumbers (cm^{-1}) of $[CH_3COSe]_2$

IR	Experimental			MP2/AUG-CC-PVDZ			Assignment
	Raman	Matrix Ar		Conf-*c*	Conf-*b*	Conf-*a*	
		Conf-*b*	Conf-*a*				
3086				3194.8 (<1.0)	3193.6 (1.6)	3188.4 (2.0)	$\nu(C–H)_{op}$
3052	3056		3010.8	3194.6 (1.7)	3187.9 (1.7)	3188.2 (1.8)	$\nu(C–H)_{op}$
3023				3165.4 (<1.0)	3168.4 (<1.0)	3164.2 (<1.0)	$\nu(C–H)_{ip}$
2964	2967			3164.8 (<1.0)	3162.0 (<1.0)	3164.1 (1.8)	$\nu(C–H)_{ip}$
2917	2917			3072.4 (<1.0)	3070.6 (<1.0)	3066.0 (<1.0)	$\nu(C–H)_{ip}$
2858	2862			3071.7 (<1.0)	3065.4 (<1.0)	3065.9 (<1.0)	$\nu(C–H)_{ip}$
1717	1720	1741.4	1746.5	1725.3 (16.1)	1741.8 (69.0)	1759.3 (100)	$\nu(C=O)_{ip}$
1684		1733.0	1736.8	1719.5 (100)	1727.9 (100)	1741.6 (76.2)	$\nu(C=O)_{op}$
			1435.7	1452.6 (3.1)	1460.1 (4.1)	1461.1 (3.5)	$\delta(H–C–H)_{ip}$
1437	1442	1423.5	1434.0	1447.2 (3.7)	1453.9 (5.2)	1460.3 (9.7)	$\delta(H–C–H)_{op}$
		1420.0	1421.9	1436.0 (4.4)	1447.4 (4.8)	1448.8 (2.7)	$\delta(H–C–H)_{ip}$
1415		1405.4	1406.6	1436.0 (1.3)	1445.5 (7.4)	1448.4 (7.9)	δ $(H–C–H)_{op}$
1370	1371	1357.2	1355.9	1362.6 (2.0)	1362.1 (6.7)	1360.6 (15.1)	δ_a $(CH_3)_{twisting}$
1350		1351.1	1349.9	1357.5 (5.0)	1355.8 (6.7)	1360.3 (3.8)	δ_s $(CH_3)_{twisting}$
		1121.8	1105.8	1131.0 (23.3)	1128.5 (50.3)	1113.3 (71.7)	$\delta_s(H–C–C)$
1098	1097	1094.9	1084.2	1116.7 (45.4)	1108.8 (67.8)	1102.4 (79.7)	$\delta_a(H–C–C)$
1021	1029		950.2	999.1 (<1.0)	1004.7 (<1.0)	1000.2 (3.8)	δ $(CH_3)_{wagging}$
999	999		945.9	993.8 (<1.0)	999.6 (1.4)	998.5 (4.3)	δ $(CH_3)_{wagging}$
943		921.6	939.4	942.9 (3.7)	953.0 (15.1)	958.0 (24.9)	$\nu_s(C–C)$
		919.7	936.4	937.0 (8.9)	944.6 (10.8)	956.8 (12.2)	ν_a (C–C)
580	580	575.4	573.7	585.8 (10.6)	582.0 (25.0)	569.3 (41.4)	$\nu_s(C–Se)$
539	542	571.2	563.9	575.5 (21.9)	567.5 (31.7)	566.3 (37.7)	ν_a (C–Se)
	505			482.7 (<1.0)	491.8 (<1.0)	491.8 (<1.0)	$\delta_{oop}(CO)_{ip}$
				466.4 (<1.0)	471.0 (<1.0)	477.5 (<1.0)	$\delta_{oop}(CO)_{op}$
	381			344.5 (<1.0)	371.1 (<1.0)	373.0 (<1.0)	$\delta(Se–C=O)_{ip}$
				327.0 (<1.0)	337.5 (<1.0)	368.9 (2.2)	$\delta(Se–C=O)_{op}$
	324			323.6 (<1.0)	324.1 (1.8)	320.6 (1.4)	$\nu(Se–Se)$
	302			321.6 (1.6)	303.2 (<1.0)	294.2 (<1.0)	$\delta(Se–C–C)_{op}$
	265			260.7 (<1.0)	257.4 (<1.0)	258.7 (1.8)	$\delta(Se–C=O)_{ip}$
				150.0 (<1.0)	167.5 (<1.0)	137.8 (1.2)	$\delta(Se–Se–C)_{op}$
				138.9 (<1.0)	133.5 (1.2)	115.0 (<1.0)	$\delta(Se–Se–C)_{ip}$
	96			132.2 (<1.0)	115.5 (1.3)	92.4 (1.4)	τ (C–Se–Se–C)
				125.2 (<1.0)	78.5 (<1.0)	75.4 (<1.0)	τ $(CH_3)_{op}$
				64.2 (<1.0)	72.7 (<1.0)	74.6 (<1.0)	τ $(CH_3)_{ip}$
				52.9 (1.1)	60.5 (<1.0)	56.5 (3.4)	τ $(H–C–C–O)_{op}$
				41.2 (<1.0)	50.5 (<1.0)	48.2 (<1.0)	τ $(H–C–C–O)_{ip}$

ip, in phase; op, out of phase.

Vibrational analysis

Vibrational properties of the molecule were tackled experimentally by recording Raman and FTIR spectra of the pure liquid (Fig. 6). Vibrational assignments, listed in Table 3, were performed with the aid of predictions of theoretical calculations and also by comparing with related molecules, that is, $CH_3C(O)SeH$[24] and $[CH_3C(O)S]_2$.[33]

Because the carbonyl stretching mode can be considered as a conformational sensor for these kinds of molecules,[24,34,35] the presence of two C=O groups in $[CH_3C(O)Se]_2$ plays a special role. Zooming in on this area (Fig. 7), it is not easy to see the signals of the two carbonyl groups separately, in either the FTIR spectrum or the FTRaman spectrum of the pure liquid. However, when the FTIR spectrum was measured for the isolated molecule in an argon matrix at low temperatures, the C=O stretching region appeared as a multiplet (top spectrum in Fig. 7). In fact, the same matrix sites were observed in all other spectral regions as well (refer to top spectrum in Fig. 8). So, the most plausible interpretation for the multiplets in the IR matrix spectrum of $[CH_3COSe]_2$, apart from cage effects, is the existence of a conformational equilibrium at room temperature,[36] thus agreeing with the theoretical predictions.

In order to check this interpretation, we performed an analysis of the multiplets in all absorption regions in the FTIR argon matrix spectrum of the molecule by considering the vibrational shifts and conformational populations predicted theoretically. As Fig. 8 shows, we found a good match between the

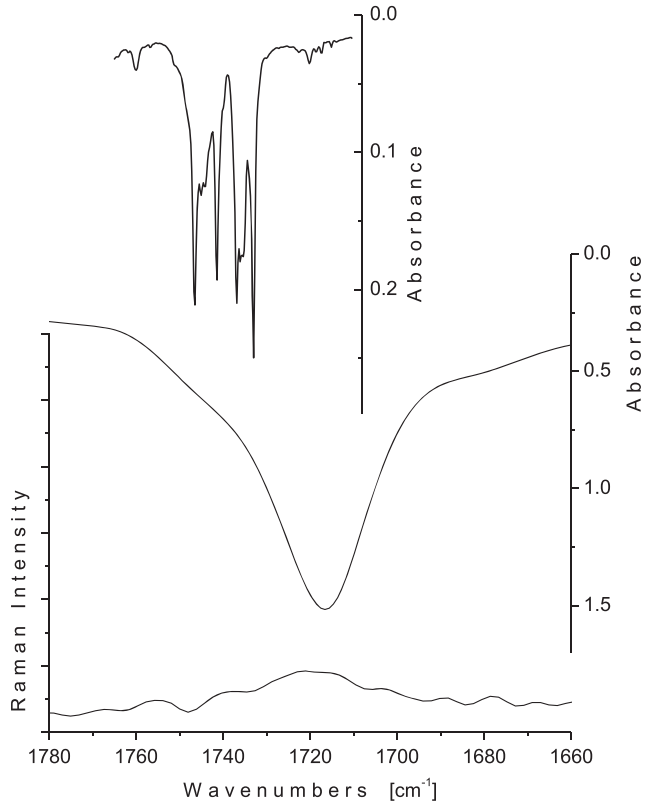

Figure 7. C=O stretching region zooming: Raman (bottom), IR (medium) and Ar matrix (top) vibrational spectra of diacetyl diselenide

experimental multiplet patterns and the calculated (MP2/aug-cc-pvdz) intensity ratios and shifts for a spectrum formed by a mixture 71/29 of conformers *a*/*b*. No signal in the argon matrix FTIR spectrum could be attributed to the less stable conformer *c*. Accordingly, we present in Table 3 a detailed assignment of the IR bands observed in solid argon for $[CH_3C(O)Se]_2$ in terms of an equilibrium between the conformers *a* and *b* at room temperature.

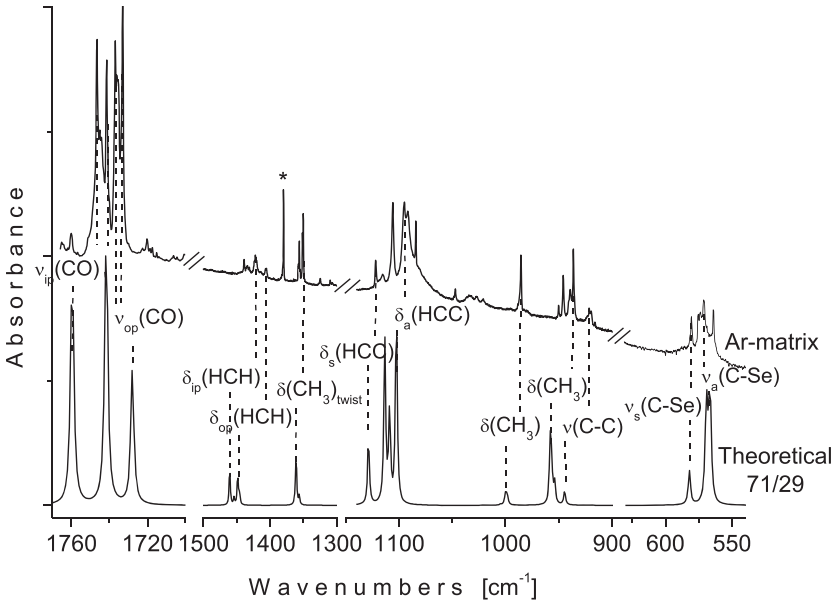

Figure 8. Comparison between the experimental Ar matrix FTIR spectrum (top) and the theoretical (MP2/aug-cc-pvdz) IR spectrum for a mixture 71/29 of conformer-a/conformer-b (bottom) of diacetyl diselenide. (Asterisk in argon matrix spectrum corresponds to an impurity of acetic acid)

Argon matrix photochemistry

Argon matrix-isolated diacetyl diselenide was exposed to UV-visible broad-band light ($200 \leq \lambda \leq 800$ nm) at different irradiation times, and changes in the IR spectrum were monitored. New absorption bands at 3060.3, 2142.2/2139.8/2138.2, 2083.7/2081.8, 2010.6 and 1374.2 cm^{-1} appeared after only 15 s of irradiation, while others at 2949.2, 1444.3, 1281.9, 979.6, 973.6 and 892.3 were better recognized after 30 s of photolysis (refer to Figures SI-1 to SI-3 in Supporting Information). All new bands were grown to the maximum period of irradiation of 60 s at the expense of a rapid depletion of bands of $[CH_3C(O)Se]_2$, suggesting a direct formation and trapping of photoproducts from this molecule (refer to Figure SI-4).

The first photoproduct to be identified was the carbonyl selenide, OCSe. At 2010.6 cm^{-1} (refer to Figure SI-2), its signal is very close to the 2009.0 cm^{-1} stretching C=O mode recently reported for the molecule isolated in an argon matrix both alone or with products derived from photodecomposition of selenoacetic acids, RC(O)SeH (R = CH_3, CF_3 or $ClCF_2$).[24,25,36,37]

The next molecule detected during the photolysis of $[CH_3C(O)Se]_2$ was ketene, $H_2C{=}C{=}O$, with its main IR absorptions appearing at 3060.3, 2142.2/2139.8/2138.2, 2083.7/2081.8, 1374.2 and 973.6 cm^{-1} for the $\nu_s(CH_2)$, $\nu(CO)$, $\nu(^{13}CO)$, $\delta(CH_2)$ and $\rho(CH_2)$ modes, respectively (Figures SI-1 and SI-3).[38] This compound was found to be the most abundant photoproduct formed from diacetyl diselenide, which is in accordance with the photochemical mechanisms proposed for the related molecules $CH_3C(O)SeH$[24] and $CH_3C(O)SX$[39] [X = –H, $–CH_3$ and $–C(O)CH_3$] isolated in argon matrices. Similar to the previously mentioned photolysis experiments, the principal clue used to distinguish the C=O stretching mode of ketene (2138.2 cm^{-1}) from those of carbon monoxide (2138.0 cm^{-1})[40] in argon matrix was its satellite $^{13}C{=}O$ vibrational band at 2081.8 cm^{-1}. This differs by about 10 cm^{-1} for the corresponding value reported at 2092.0 cm^{-1} for the CO molecule.

Finally, another photochemical product to be identified was methylselane, CH_3SeH. The formation of this compound is consistent not only from the stoichiometric point of view but is also in agreement with the photo-made bands previously reported for CH_3SeH in argon matrix,[41] as well as the identified CH_3EH (E = S or Se) species during the photoevolution of the related $CH_3C(O)SeH$[24] and $CH_3C(O)SX$ [X = –H, $–CH_3$ and $–C(O)CH_3$][39] molecules.

Table 4 lists the band position and assignment of the IR absorptions appearing after photolysis of $[CH_3C(O)Se]_2$ in solid argon, along with the wavenumbers reported previously also in Ar matrix for the proposed photoproducts. Based on the identity of the photoproducts, we propose the following photochemical path for the molecule of diacetyl diselenide isolated in an argon matrix (Scheme 2).

Table 4. Band position (in cm^{-1}) and assignment of the IR absorptions appearing after photolysis of $[CH_3COSe]_2$ isolated in solid argon

Wavenumbers	Molecule	Mode	Wavenumbers reported previously
3060.3	H_2CCO	$\nu_s(CH_2)$	3062.5[a]/3062[b]
2949.2	CH_3SeH	$\nu_a(CH)$	2949.4[a]/2987[c]
2142.2/2139.8/2138.2/2136	H_2CCO	$\nu(CO)$	2145.2[a]/2138.4[a]/2138.1[a]/2136.2[a]/2142[b]
2083.7/2081.8	H_2CCO	$\nu(^{13}CO)$	2082.1[a]/2081.6[a]/2085[b]
2014.8/2010.6/2006.9	OCSe	$\nu(CO)$	2009.0[ad]
1444.3	CH_3SeH	$\delta_a(CH_3)$	1444.3[a]/1438[c]
1374.2	H_2CCO	$\delta(CH_2)$	1375.0[a]/1374.3[a]/1381[b]
1281.9	CH_3SeH	$\delta_s(CH_3)$	1281.9[a]/1275[c]
979.6	CH_3SeH	$\rho(CH_3)$	979.2[a]/982[c]
973.6	H_2CCO	$\rho(CH_2)$	973.6[a]/974[b]
892.3	CH_3SeH	$\rho(CH_3)$	896.3[a]/918[c]

[a]Reference [24].
[b]Reference [39].
[c]Reference [41].
[d]Reference [37].

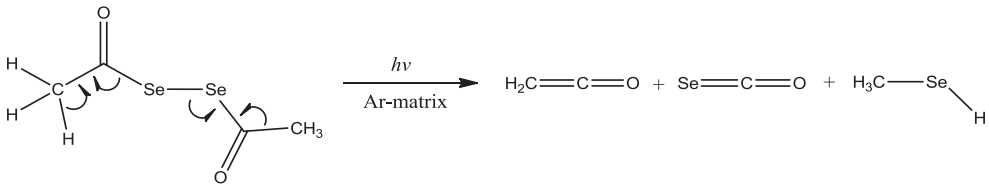

Scheme 2. Proposed photolysis reaction for diacetyl diselenide isolated in solid argon

CONCLUSION

We have carried out preparation, mass fragmentation, vibrational characterization and Ar matrix photodecomposition of diacetyl diselenide, $CH_3C(O)SeSeC(O)CH_3$, for the first time. The novel compound was obtained by treating pure selenoacetic acid, $CH_3C(O)SeH$, with oxygen. The conformational behavior of diacetyl diselenide was approached by means of a combined theoretical/matrix isolation study. From this, it was possible to rationalize its gas phase composition at room temperature as an equilibrium mixture between two structures; these are denoted in this work as conformers *a*(C_2) and *b*(C_1). According to our B3LYP/6-311++G(3df,3pd) or MP2/aug-cc-pvdz calculations, C_2 form is more stable than the C_1 by 0.18 or 0.42 kcal/mol, respectively. Major thermochemical stability of conformer *a* was interpreted theoretically, using an NBO analysis. More efficient delocalization energy coming from vicinal hyperconjugative interactions implies lone pairs on selenium or oxygen atoms and C=O, C–C or Se–C antibonding orbitals. Exposure of a molecule of $CH_3C(O)SeSeC(O)CH_3$, isolated in argon cage at low temperatures, to a UV-vis radiation of broad band ($200 \leq \lambda \leq 800$ nm) led to a rapid photolysis of the compound to bring about ketene, $H_2C{=}C{=}O$, and CH_3SeH and OCSe.

Acknowledgements

J.A.G.C. thanks Universidad Pedagógica y Tecnológica de Colombia (UPTC) for financial support for the Project SGI 1535 of Dirección de Investigaciones (DIN) and Deutscher Akademischer Austausch Dienst (DAAD) for the PhD award during his studies in La Plata. C.O.D.V and R.M.R. acknowledge Consejo Nacional de Investigaciones Científicas y Técnicas (CONICET), Facultad de Ciencias Exactas, Universidad Nacional de La Plata and ANPCyT for financial support.

REFERENCES

[1] J. Beld, K. J. Woycechowsky, D. Hilvert, *J. Biotechnol.* **2010**, *150*, 481.
[2] D. Plano, Y. Baquedano, D. Moreno-Mateos, M. Font, A. Jiménez-Ruiz, J. A. Palop, C. Sanmartín, *Eur. J. Med. Chem.* **2011**, *46*, 3315.
[3] A. Sausen de Freitas, J. B. Teixeira Rocha, *Neurosci. Lett.* **2011**, *503*, 1.
[4] F. B. Zasso, C. E. P. Goncales, E. A. C. Jung, D. Araldi, G. Zeni, J. B. T. Rocha, C. W. Nogueira, *Environ. Toxicol. Pharmacol.* **2005**, *19*, 283.
[5] A. M. Favero, S. N. Weis, G. Zeni, J. B. T. Rocha, C. W. Nogueira, *Neurotoxicol. Teratol.* **2006**, *28*, 607.
[6] N. B. V. Barbosa, J. B. T. Rocha, D. C. Wondracek, J. Perottoni, G. Zeni, C. W. Nogueira, *Chem. Biol. Interact.* **2006**, *163*, 230.
[7] R. B. Raffa, *Life Sci.* **2010**, *87*, 451.
[8] T. Fiuza, C. S. Oliveira, M. da Costa, V. A. Oliveira, G. Zeni, M. E. Pereira, *J. Trace Elem. Med. Biol.* **2015**, *29*, 255.
[9] S. Terra Stefanello, P. Gubert, B. Puntel, C. Rigon Mizdal, M. M. Anraku de Campos, S. M. Salman, L. Dornelles, D. Silva Avila, M. Aschner, F. A. Antunes Soares, *Toxicol. Rep.* **2015**, *2*, 961.
[10] V. Nascimento, N. L. Ferreira, R. F. S. Canto, K. L. Schott, E. P. Waczuk, L. Sancineto, C. Santi, J. B. T. Rocha, A. L. Braga, *Eur. J. Med. Chem.* **2014**, *87*, 131.
[11] D. Kaur, P. Sharma, P. V. Bharatam, *J. Mol. Struc. Theochem.* **2007**, *810*, 31.
[12] K. Ajiki, M. Hirano, K. Tanaka, *Org. Lett.* **2005**, *7*, 4193.
[13] A. L. Braga, P. H. Schneider, M. W. Paixao, A. M. Deobald, *Tetrahedron Lett.* **2006**, *47*, 7195.
[14] G. Tabarelli, E. E. Alberto, A. M. Deobald, G. Marin, O. E. D. Rodrigues, L. Dornelles, A. L. Braga, *Tetrahedron Lett.* **2010**, *51*, 5728.

[15] N. L. Ferreira, J. B. Azeredo, B. L. Fiorentin, A. L. Braga, *Eur. J. Org. Chem.* **2015**, *2015*, 5070.
[16] B. M. Vieira, S. Thurow, J. S. Brito, G. Perin, D. Alves, R. G. Jacob, C. Santi, E. J. Lenardão, *Ultrason. Sonochem.* **2015**, *27*, 192.
[17] R. Dubey, H. Lee, D. Nam, D. Lim, *Tetrahedron Lett.* **2011**, *52*, 6839.
[18] E. Moreno, D. Plano, I. Lamberto, M. Font, I. Encio, J. A. Palop, C. Sanmartin, *Eur. J. Med. Chem.* **2012**, *47*, 283.
[19] Y. Hou, A. Z. Rys, I. A. Abu-Yousef, D. N. Harpp, *Tetrahedron Lett.* **2003**, *44*, 4279.
[20] Y. Gong, K. Shimada, H. Nakamura, M. Fujiyama, A. Kodama, M. Otsuki, R. Matsumoto, S. Aoyagi, Y. Takikawa, *Heteroatom Chem.* **2006**, *17*, 125.
[21] J.-X. Wang, L. Bai, Z. Liu, *Synth. Commun.* **2000**, *30*, 971.
[22] S. Kumar, S. K. Tripathi, H. B. Singh, G. Wolmershäuser, *J. Organomet. Chem.* **2004**, *689*, 3046.
[23] T. Takahashi, O. Niyomura, S. Kato, M. Ebihara, *Z. Anorg. Allg. Chem.* **2013**, *639*, 108.
[24] J. A. Gómez Castaño, R. M. Romano, H. Beckers, H. Willner, R. Boese, C. O. Della Védova, *Angew. Chem. Int. Ed.* **2008**, *47*, 10114.
[25] J. A. Gómez Castaño, R. M. Romano, H. Beckers, H. Willner, C. O. Della Védova, *Inorg. Chem.* **2010**, *49*, 9972.
[26] M. J. Almond, A. J. Downs, *Advances in Spectroscopy 17* Wiley, Chichester, **1989**.
[27] I. R. Dunkin, *Matrix-Isolation Techniques: A Practical Approach*, Oxford University Press, New York, **1998**.
[28] R. N. Perutz, J. J. Turner, *J. Chem. Soc. Faraday Trans.* **1973**, *69*, 452.
[29] M. J. Frisch, G. W. Trucks, H. B. Schlegel, G. E. Scuseria, M. A. Robb, J. R. Cheeseman, G. Scalmani, V. Barone, B. Mennucci, G. A. Petersson, H. Nakatsuji, M. Caricato, X. Li, H. P. Hratchian, A. F. Izmaylov, J. Bloino, G. Zheng, J. L. Sonnenberg, M. Hada, M. Ehara, K. Toyota, R. Fukuda, J. Hasegawa, M. Ishida, T. Nakajima, Y. Honda, O. Kitao, H. Nakai, T. Vreven, J. A. Montgomery Jr., J. E. Peralta, F. Ogliaro, M. Bearpark, J. J. Heyd, E. Brothers, K. N. Kudin, V. N. Staroverov, T. Keith, R. Kobayashi, J. Normand, K. Raghavachari, A. Rendell, J. C. Burant, S. S. Iyengar, J. Tomasi, M. Cossi, N. Rega, J. M. Millam, M. Klene, J. E. Knox, J. B. Cross, V. Bakken, C. Adamo, J. Jaramillo, R. Gomperts, R. E. Stratmann, O. Yazyev, A. J. Austin, R. Cammi, C. Pomelli, J. W. Ochterski, R. L. Martin, K. Morokuma, V. G. Zakrzewski, G. A. Voth, P. Salvador, J. J. Dannenberg, S. Dapprich, A. D. Daniels, Ö. Farkas, J. B. Foresman, J. V. Ortiz, J. Cioslowski, D. J. Fox, *Gaussian 09, Revision C.01*, Gaussian, Inc., Wallingford CT, **2010**.
[30] E. D. Glendening, A. E. Reed, J. E. Carpenter, F. Weinhold, *NBO Version 3.1*, Madison, WI, **1998**.
[31] R. Dennington, T. Keith, J. Millam, *GaussView, Version 5*, Semichem Inc., Shawnee Mission, KS, **2009**.
[32] J. Robert, M. Anouti, M. Abarbri, J. Paris, *J. Chem. Soc. Perkin Trans.2*. **1997**, 1759.
[33] A. J. Speziale, C. C. Tung, *J. Org. Chem.* **1963**, *28*, 1353.
[34] R. M. Romano, C. O. Della Védova, A. J. Downs, H. Oberhammer, S. Parsons, *J. Am. Chem. Soc.* **2001**, *123*, 12623.
[35] L. C. Juncal, M. V. Cozzarín, R. M. Romano, *Spectrochim. Acta Mol Biomol. Spectrosc.* **2015**, *139*, 346.
[36] J. A. Gómez Castaño, R. M. Romano, *Vib. Spectrosc.* **2014**, *70*, 28.
[37] J. A. Gómez Castaño, R. M. Romano, H. Beckers, H. Willner, C. O. Della Védova, *Eur. J. Inorg. Chem.* **2013**, *2013*(26) 4585.
[38] C. B. Moore, G. C. Pimentel, *J. Chem. Phys.* **1963**, *38*, 2816.
[39] R. M. Romano, C. O. Della Védova, A. J. Downs, *J. Phys. Chem. A.* **2002**, *106*, 7235.
[40] H. Dubost, *Chem. Phys.* **1976**, *12*, 139.
[41] A. B. Harvey, M. K. Wilson, *J. Chem. Phys.* **1966**, *45*, 678.

SUPPORTING INFORMATION

Additional supporting information may be found in the online version of this article at the publisher's website.